Mathematical Modelling in Medicine and Public Health Coursework 2025

Guy Davies
zm21678@bristol.ac.uk
github.com/guydavies02/MathModellinginHealth

March 26, 2025

1 Introduction

1.1 Biological Background

Hasty et al. (2002) [4] proposed a synthetic gene oscillator, with the goal of amplifying natural oscillations in cells. This represented an important advancement, as if a gene regulatory network (GRN) can be coupled with a biological system, it could be used in designing integrated biological circuits and lead to controlling cellular function and development.

The synthetic oscillator is constructed using two plasmids, both containing the same promoter. On the first plasmid, this promoter controls the cI gene, regulating the expression of CI protein. On the second plasmid, the promoter controls the lac gene, regulating the production of Lac protein.

The core of this system relies on two critical binding configurations that affect transcription rates:

- When a CI dimer binds to the OR2 operator site while the OR3 site remains vacant, the promoter is "turned on," causing increased transcription of its gene.
- When a Lac tetramer binds to the OR3 operator site, the promoter is "turned off," inhibiting transcription.

These interactions create a feedback system where CI activates its own production (positive feedback) while Lac inhibits the production of both proteins (negative feedback). This combination of positive and negative feedback loops is what enables the system to generate oscillatory dynamics.

Two equations are given initially for the system

$$\frac{dX}{d\tau} = -2k_1X^2 + 2k_{-1}X_2 + k_t\left(D^1 + D^1X_2 + aD^1X_2X_2\right) - k_xX,$$

$$\frac{dY}{d\tau} = -2k_2Y^2 + 2k_{-2}Y_2 + k_t\left(D^2 + D^2X_2 + aD^2X_2X_2\right) - k_yY,$$

where X and Y denote the concentration of CI and Lac respectively and the terms in brackets represent the concentrations of DNA and DNA-protein complexes of plasmids 1 and 2. These equations are further simplified by utilising the assumption that timescales can be separated, as multimerisation processes (where proteins combine to form dimers and tetramers) happen much faster than transcription and degradation. Dimensionless variables are used to reduce the equations to

$$\frac{dx}{dt} = \frac{1 + x^2 + \alpha\sigma x^4}{(1 + x^2 + \sigma x^4)(1 + y^4)} - \gamma_x x$$

$$\tau_y \frac{dy}{dt} = \frac{1 + x^2 + \alpha\sigma x^4}{(1 + x^2 + \sigma x^4)(1 + y^4)} - \gamma_y y$$

where α represents the degree to which the transcription rate is increased when a CI dimer is bound to OR2, and σ is the affinity for a CI dimer binding to OR2 relative to binding at OR1. γ_x and γ_y denote the degradation rate of the CI and Lac proteins respectively, and are taken to be tunable as they can be changed by varying temperature.

This translation to a dimensionless form is useful as it reduces the parameter space, allowing us to see more direct changes in system behaviour and making each of them more interpretable. For example, α directly represents the activation strength of CI, rather than a combination of many rate constants which are difficult to determine.

2 Literature Review

This influential paper from Hasty et al. was impactful as it presented a model for a synthetic gene oscillator, explored its coupling to intrinsic cellular oscillations, and began to investigate its synchronisation properties, providing a framework for entraining and amplifying oscillations in cellular protein levels. The concept of designing synthetic gene oscillators dates back to the work of Goodwin (1963) [3], who proposed a simple model for self-repressing gene expression. Though this was one of the first synthetic genetic oscillators to be studied, it was also the simplest oscillator, comprising a single gene that represses itself. Models using this suggested that oscillations could arise through a Hopf bifurcation, however they were irregular and often unpredictable, limiting the utility of the design.

During the decades following Goodwin's oscillator, synthetic gene oscillators slowly developed but without the major breakthroughs which would lead to robust and tunable oscillators. This came in when Smolen et al. (1998) [5] presented a model with two genes, where one gene promoted its transcription and that of the other, while the second gene repressed its transcription and that of the first. While both positive and negative feedback loops where present here, the resulting dynamics where less complex than those of Hasty et al. (2002). Smolen et al. examined biological GRNs and described their workings, which were then expanded on to design the synthetic oscillator found in Hasty et al. (2002). As a result of its complexity, the Hasty oscillator was more capable of amplifying cellular oscillations. This improved its potential utility and therefore proved its impact in the field

Other models at the time included the three gene repressilator[2], which demonstrated that synthetic oscillators could function in living cells, but Hasty et al. (2002) introduced a

two-plasmid design that offered key improvements. By using a shared promoter to regulate CI and Lac, their model enhanced robustness and linked synthetic oscillations to natural cellular processes. This enabled entrainment and amplification. Unlike the repressilator, which relied solely on negative feedback and lacked synchronisation mechanisms, Hasty et al.'s design allowed for finer control and external tuning, making it more useful for real-world applications.

Amplified negative feedback oscillators operate differently, with one gene activating itself and a second gene, which then represses the first, originally proposed in Atkinson et al. (2003)[1]. These systems rely on fast activation and degradation, producing high-frequency oscillations with more linear repression than Hasty et al.'s transcription. This contributes to stochastic coherence, contrasting with the subcritical dynamics of Hasty's model. Despite these differences, Hasty's oscillator expanded the tunable design space, enabling precise control over cellular signals and protein levels.

Subsequent studies have built upon Hasty et al.'s framework to explore how different circuit architectures and parameter tuning can affect the oscillatory period. For example, Stricker et al. (2008)[6] engineered a faster synthetic gene oscillator, owing in part to the understanding of the Hasty network and its architecture. Improved tunability allowed it to reach a period of as low as 13 minutes. One key difference is that it exhibited more complex dynamics by using a higher dimensional model leading to two limit cycles existing simultaneously. Richer dynamics are desirable because a more versatile and capable oscillator has more potential use cases in biology. For example, simultaneous limit cycles could allow the GRN to switch between different oscillatory modes based on environmental conditions.

Hasty et al. (2002) focused on a specific implementation of the oscillator and its mathematical analysis, Tsai et al. (2008)[8] discussed design principles more generally. They showed specifically that interlinked positive and negative feedback yields specific performance benefits. It gives synthetic biologists a valuable blueprint for designing oscillators with predictable and desirable characteristics. Another interesting aspect of the paper is its explanation of why certain natural systems use similar combinations of positive and negative feedback. This rationalises the synthetic models in relation to the biological systems they are designed to couple with. Overall, Tsai et al. (2008) backed up the foundations of the oscillator in Hasty et al. (2002), providing a more concrete and explainable connection between the network topology and oscillatory behaviour.

The model has also served as a basis for the development of eukaryotic oscillators. Tigges et al. (2009)[7] built upon the ideas in Hasty et al. (2002) but advanced to synthetic mammalian systems. Previously, synthetic oscillators had been mostly limited to prokaryotic cells, however expanding to eukaryotic systems has more real world use, as they can be applied to human cells and diseases.

3 Model Analysis

3.1 Temporal Dynamics

The model can be simulated to show the oscillatory dynamics. My allocated parameter is γ_x, the degradation factor of CI protein. While this is the parameter varied for the majority of the following analysis, I have also included some variation of others.

For default parameters, α and σ are set as 11 and 2, and are chosen empirically. They represent the impact and likelihood of a CI dimer binding to OR2, as mentioned above. While τ_y is a design parameter, it has been set to 5 as this is consistent with values used for dimensionless forms with these proteins. As shown below, as well as in the paper, values of γ_y up to around 0.037 lead to oscillations, with higher values giving damping effects. Therefore when varying γ_x for my analysis, I will use a value of $\gamma_y = 0.036$ in order to encourage interesting dynamics. When varying γ_y, a value of $\gamma_x = 0.15$ is used, as oscillations are found when this is around 3 times bigger than γ_y. Choosing and varying values for degradation factors is reasonable they are adjustable for both proteins by varying the temperature.

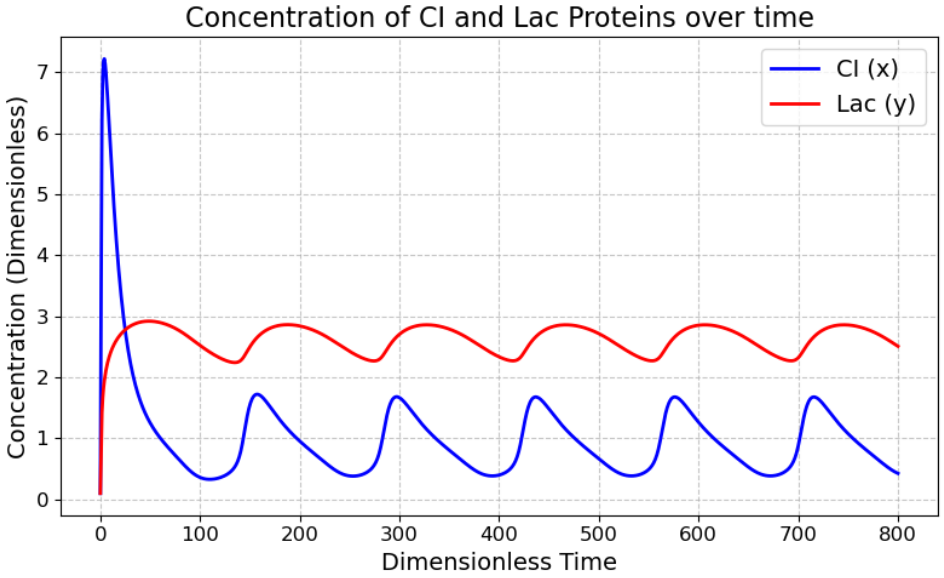

Figure 1: Simulated behaviour of the dimensionless system showing concentrations of CI and Lac proteins over time. Clear stable oscillations arise. Parameter values used are $\gamma_x = 0.105, \gamma_y = 0.036, \alpha = 11, \sigma = 2, \tau_y = 5$.

As mentioned in the literature review, Hasty et al's paper was influential because it showed a stable, tunable and robust oscillatory system. Figure 1 shows these oscillations along with the spike in CI concentration which initialises them. Notably, oscillations of one protein require oscillations of the other, they can only coexist. Therefore in all further analysis I will only be observing changes in CI concentration, denoted as X. However, all conclusions and parameter values apply similarly to Lac concentration.

3.2 Parameter Variation

To better understand the dynamics of the system and the conditions for tunable oscillations, we must further analyse the effects of the parameters we are most in control of, the degradation factors. I will analyse γ_x, but it is worth noting that changes to γ_y can give a similar effect. The ratio of these is key to sustaining oscillations.

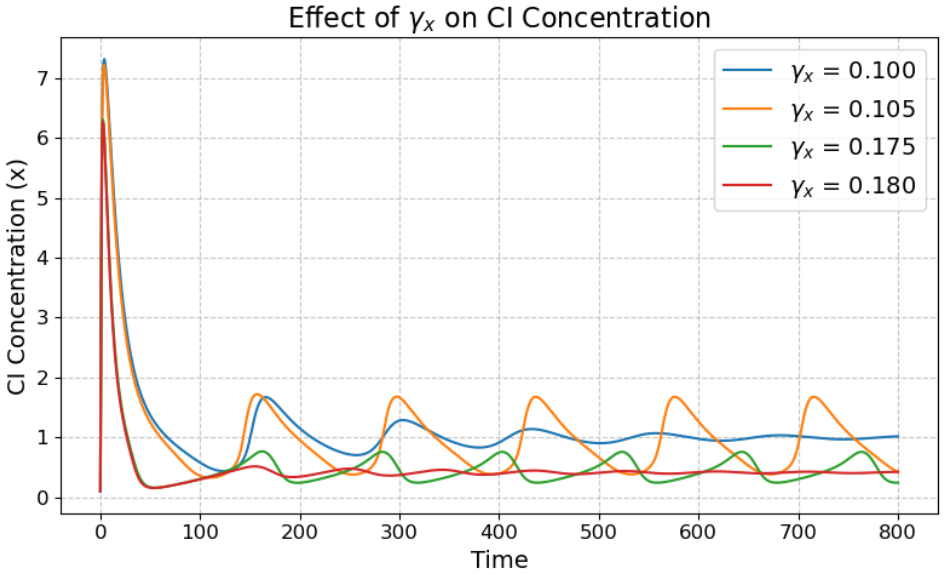

Figure 2: CI concentration over time for a range of γ_y values. The range of γ_x which sustain oscillations is shown to be from 0.105 to around 0.175. Parameter values used are $\gamma_y = 0.036, \alpha = 11, \sigma = 2, \tau_y = 5$.

By varying γ_x, we can approximate the window of values for which oscillatory behaviour emerges, as shown in Figure 2. While oscillations are visible for $\gamma_x = 0.1$, damping effects cause them to die out. It is not until a value of around 0.105 that the oscillations become stable. Additionally, while the nature of the nature of the oscillations changes significantly, they are stable until γ_x reaches approximately 0.175, after which significant damping causes them to die out very quickly.

Also from the figure, we can see how amplitude and frequency can be tuned. Increasing γ_x increases the frequency of the oscillations, but decreases amplitude. This is because a higher degradation rate lowers the concentration of CI protein, even whilst oscillations are present. Frequency changes because when the maximum build up of CI protein is lower, less time is needed for the repressive effects of Lac protein to bring it down. This trend increases until oscillations die out when $\gamma_x = 0.18$. The equilibrium reached at this point is much lower than the equilibrium before oscillations are stable because the higher degradation rate decreases CI concentration.

As mentioned in the paper, oscillations are favoured when the degradation rate for CI is 2-3 times higher than that of Lac. If γ_x is too low, CI proteins are not degrading very quickly, meaning the system dynamics are imbalanced. CI proteins persist in the system for too long, disrupting the oscillatory behaviour and driving the system to a steady state. Conversely, a higher degradation rate prevents CI from reaching a sufficient level to repress Lac transcription, causing Lac to dominate the system. Fundamentally, changes to either degradation rate affects the phase difference of X and Y, so there is not a large enough build up of one protein to bring down the concentration of the other, thereby preventing oscillations.

The effects of γ_x are inherently linked to γ_y, as changing either can disrupt the phase of their respective concentrations, which in turn prevents oscillations.

4 Phase Plane Analysis

Using the values found from plotting time series for varying γ_x values in the previous section, phase planes can be examined to further analyse the system's behaviour.

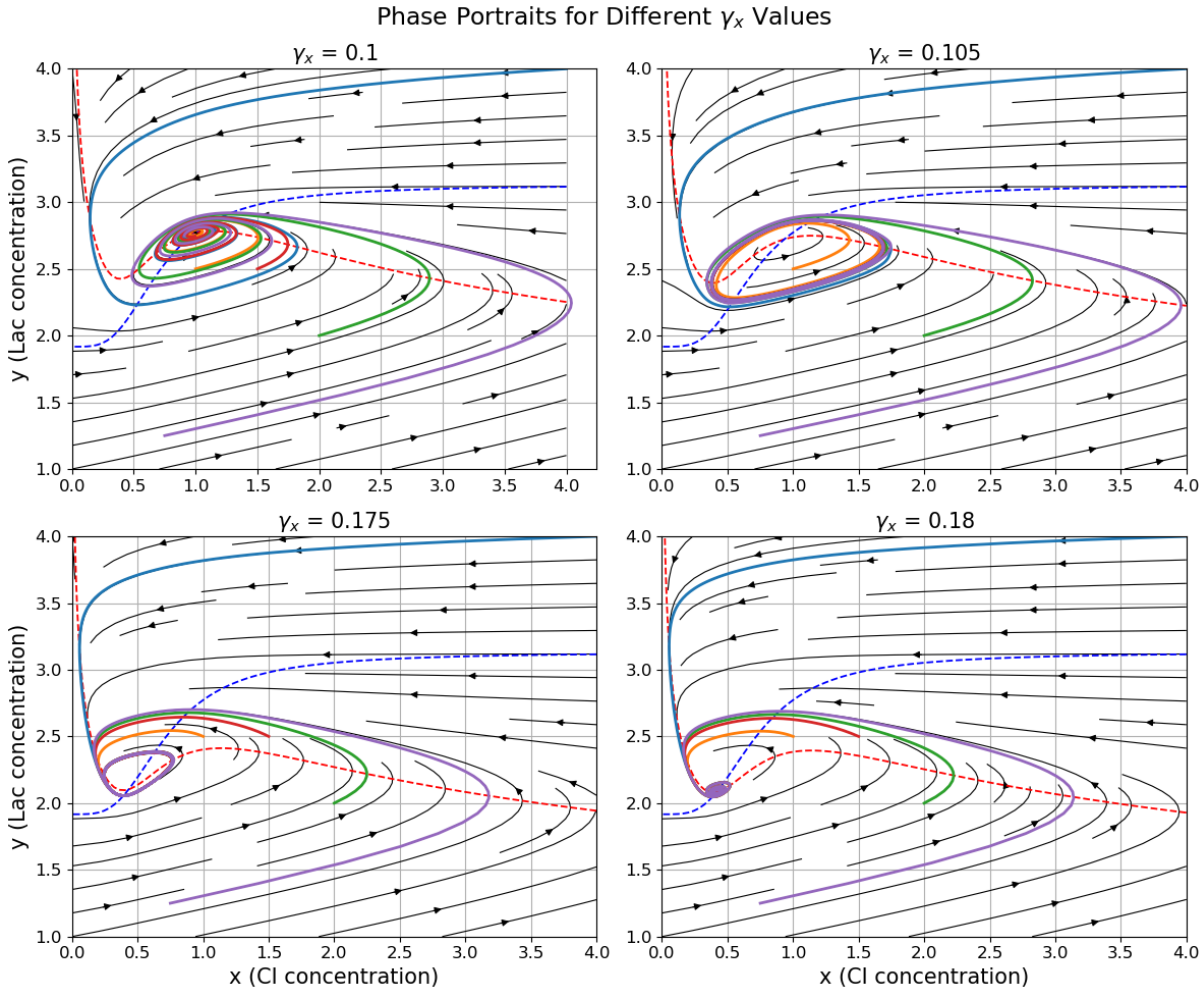

Figure 3: Phase plane analysis showing nullclines, equilibria, and trajectories for γ_x close to Hopf bifurcations. Dotted lines show nullclines, and coloured lines show trajectories. Parameter values used are $\gamma_y = 0.036, \alpha = 11, \sigma = 2, \tau_y = 5$.

Stable limit cycles arise when using γ_x values within a critical range of approximately 1.05-1.75. Figure 3 shows stable fixed point equilibriums for values below and above this range, indicating the presence of Hopf bifurcations. All trajectories shown spiral towards the limit cycles, demonstrating their stability. This shows the robustness of the oscillator against perturbations or varied initial conditions, which is an important trait for biological applications where noise and fluctuations are inevitable. Additionally, the phase planes have symmetry, reinforcing the idea that neither protein can oscillate independently as mentioned previously.

The nullclines can also give insight into the system dynamics. The intersections of the nullclines define equilibrium points, and the nature of these equilibria varies depending on the degradation rate parameters. When γ_x is tuned near the Hopf bifurcation, as in Figure 3, small changes lead to the transition between steady-state and oscillatory

behaviour. This suggests that the system is highly sensitive to degradation rates, which aligns with the biological reality that protein stability and degradation play a crucial role in regulating gene expression oscillations.

When γ_x first enters critical region causing oscillations, at a value of around 0.105, the system suddenly goes from a single fixed point equilibrium to a relatively large limit cycle. This suggests there could be bistability or a Canard explosion close to this Hopf bifurcation. The limit cycles also show how increasing γ_x decreases amplitude, as the limit cycle reduces in size until it reaches a fixed point. It is worth noting that this transition is smoother, suggesting a supercritical Hopf bifurcation.

5 Bifurcation Analysis

Further investigation is needed to fully understand the nature of the Hopf bifurcations which give rise to oscillations.

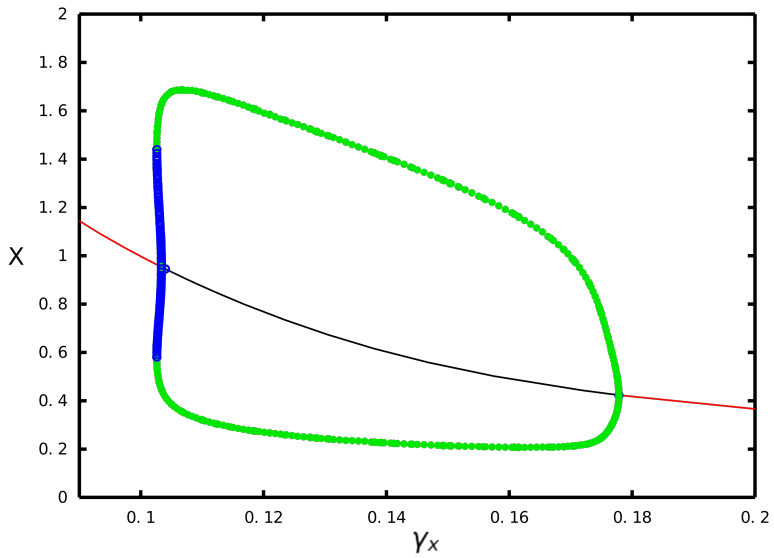

Figure 4: Bifurcation diagram using γ_x as the free parameter and CI concentration (x) as the state variable. Red and black lines denote stable and unstable fixed point equilibria, and green and blue points denote stable and unstable limit oscillations. Parameter values used are $\gamma_y = 0.036, \alpha = 11, \sigma = 2, \tau_y = 5$.

As with the phase plane, the bifurcation diagram shows a sudden jump from a stable fixed point to large oscillations. Figure 4 shows the an unstable limit cycle in blue arising from a fixed point, showing the existence of a subcritical Hopf bifurcation. A slight 'overhang' of the limit cycle can be seen, allowing for a small bistable region around approximately $\gamma_x = 0.102$, where a stable limit cycle and fixed point coexist in the system for a single parameter value. In this case, the behaviour of the system depends on whether γ_x is increasing or decreasing up to that point. While this sort of behaviour could be useful for tuning a synthetic oscillator, this region is likely too small to feasibly use for *in silico* or *in vivo* implementation.

After the initial Canard explosion, giving large oscillations from an exponentially small change in the degradation rate, we see that amplitude smoothly decreases as γ_x increases. At a value of approximately 0.178, and following a gradual decrease in size, the oscillations cease to exist and instead a single fixed point equilibrium is reached. This Hopf bifurcation is supercritical, as the limit cycle stays stable until the bifurcation is reached.

The stability of the limit cycles represents sustained oscillations, proving the robustness of the synthetic GRN. While there are fixed point equilibria within the limit cycle, they are unstable, so any slight perturbation leads to oscillatory behaviour. Due to the natural noise in biological systems, it is very unlikely that the system would remain in these unstable equilibria for long. Figure 4 also shows how γ_x can be effectively tuned to control the amplitude and frequency of oscillation, as the limit cycle smoothly changes shape.

6 Conclusion

In their groundbreaking paper, Hasty et al. detailed the implementation of a GRN capable of entraining and amplifying protein levels, and discussed coupling mechanisms to for use with CI and Lac proteins. The oscillations it produced were robust and tunable, giving it significant potential for real-world use. Importantly, they showed that certain parameters can be used in tuning the oscillations and analysed the dynamics of the system.

In this report, I have carried out similar analysis by varying the degradation factor of CI protein, γ_x. This choice of parameter is reasonable as degradation rates can be altered by a change in temperature. My analysis showed that a window of stable oscillations emerge with a γ_x value of approximately 0.102-0.178, and that within this window, increasing γ_x yields smaller oscillations with a higher frequency.

AI Usage Statement

Only spelling and grammar tools were used in this project.

References

[1] Mariette R. Atkinson, Michael A. Savageau, Jesse T. Myers, and Alexander J. Ninfa. Development of genetic circuitry exhibiting toggle switch or oscillatory behavior in Escherichia coli. *Cell*, 113(5):597–607, May 2003.

[2] M. B. Elowitz and S. Leibler. A synthetic oscillatory network of transcriptional regulators. *Nature*, 403(6767):335–338, January 2000.

[3] Brian C. Goodwin. *Temporal organization in cells; a dynamic theory of cellular control processes*. London, New York, Academic Press, 1963.

[4] Jeff Hasty, Milos Dolnik, Vivi Rottschäfer, and James J. Collins. Synthetic gene network for entraining and amplifying cellular oscillations. *Physical Review Letters*, 88(14):148101, April 2002.

[5] Paul Smolen, Douglas A. Baxter, and John H. Byrne. Frequency selectivity, multistability, and oscillations emerge from models of genetic regulatory systems. *American*

Journal of Physiology-Cell Physiology, 274(2):C531–C542, February 1998. Publisher: American Physiological Society.

[6] Jesse Stricker, Scott Cookson, Matthew R. Bennett, William H. Mather, Lev S. Tsimring, and Jeff Hasty. A fast, robust and tunable synthetic gene oscillator. *Nature*, 456(7221):516–519, November 2008.

[7] Marcel Tigges, Tatiana T. Marquez-Lago, Jörg Stelling, and Martin Fussenegger. A tunable synthetic mammalian oscillator. *Nature*, 457(7227):309–312, January 2009. Publisher: Nature Publishing Group.

[8] Tony Yu-Chen Tsai, Yoon Sup Choi, Wenzhe Ma, Joseph R. Pomerening, Chao Tang, and James E. Ferrell. Robust, tunable biological oscillations from interlinked positive and negative feedback loops. *Science (New York, N.Y.)*, 321(5885):126–129, July 2008.

7 Appendix

For the majority of the code, I used python. The system equations were defined, returning respective derivatives. I used the solve_ivp function from scipy to solve it and could then easily plot the time series, including the plot with parameter variation. For clean code, I defined the system and functions in a python file and then called them in a notebook to make it easier to interact with them.

For the phase portraits, I encountered bugs using these functions so I redefined the system slightly differently which worked much better. Nullclines are found by selecting for dx/dt =0, and dy/dt=0. I used a quiver plot to show the vector field of derivatives for both state variables. Finally, some trajectories were also added to the plot to show how initial conditions converge.

XPP was used for the bifurcation diagram. System equations and parameters were defined in a .ode file, then by opening that in XPP I could plot the phase plane and find an unstable equilibrium, which I then used as an initial point for bifurcation analysis. Then my allocated variable, γ_x, was varied to see the results on system equilibria and oscillations, finally leading to the bifurcation diagram showed.